



**Original citation:**

Reyes-Aldasoro, C. C. (2004) A guide to co-occurrence matrix analysis. University of Warwick. Department of Computer Science. (Department of Computer Science Research report).

**Permanent WRAP url:**

<http://wrap.warwick.ac.uk/61393>

**Copyright and reuse:**

The Warwick Research Archive Portal (WRAP) makes this work by researchers of the University of Warwick available open access under the following conditions. Copyright © and all moral rights to the version of the paper presented here belong to the individual author(s) and/or other copyright owners. To the extent reasonable and practicable the material made available in WRAP has been checked for eligibility before being made available.

Copies of full items can be used for personal research or study, educational, or not-for-profit purposes without prior permission or charge. Provided that the authors, title and full bibliographic details are credited, a hyperlink and/or URL is given for the original metadata page and the content is not changed in any way.

**A note on versions:**

The version presented in WRAP is the published version or, version of record, and may be cited as it appears here. For more information, please contact the WRAP Team at: [publications@warwick.ac.uk](mailto:publications@warwick.ac.uk)



<http://wrap.warwick.ac.uk/>

# A Guide to Co-occurrence Matrix Analysis

Constantino Carlos Reyes-Aldasoro

February 2004

Department of Computer Science, The University of Warwick.

## ABSTRACT

This report considers the analysis of the co-occurrence matrix that has been widely used in many texture analysis problems. The co-occurrence matrix was first presented by Haralick [4, 3] and since then, many researches have used it in a variety of applications. Though simple in concept and powerful, it has a great computational burden, first for the size of the matrix depends on the number of grey levels of the original image, second because of the number of features that can be extracted from the matrix. Many of these features would not be useful at a discrimination process. The report focuses in the analysis of the matrices and features for several binary and natural textures. Finally a human knee MRI is segmented with a set of features that is selected with the use of the Bhattacharyya distance as a measure of discrimination.

**Keywords:** Texture, Co-occurrence matrix, Joint Statistics, Image Segmentation, Discrimination.

# Contents

<b>1</b>	<b>The Co-occurrence Matrix</b>	<b>4</b>
<b>2</b>	<b>Synthetic and Natural Textures</b>	<b>6</b>
2.1	Guide to the Textures and their Results . . . . .	6
2.2	Co-occurrence Matrices of the Binary Textures . . . . .	9
2.3	Co-occurrence Matrices of the Knee Texture Examples . . . . .	11
<b>3</b>	<b>Feature Spaces by blocks for Knee Textures</b>	<b>13</b>
3.1	Example 17 : Background . . . . .	15
3.2	Example 18 : Muscle . . . . .	16
3.3	Example 19 : Bone . . . . .	17
3.4	Example 20 : Tissue . . . . .	18
3.5	Bhattacharyya distances for pairs of data . . . . .	19
3.6	15 Features of Matrices by blocks from the Human Knee MRI . . . . .	22
<b>4</b>	<b>Classification Results based on Bhattacharyya distances for pairs of data</b>	<b>25</b>

## List of Figures

1	Human knee MRI and four selected regions. . . . .	6
2	(a) Bhattacharyya distances for the 6 combinations of 4 anatomical structures. Block size 4. (b) Values greater than 0.15 . . . . .	19
3	(a) Bhattacharyya distances for the 6 combinations of 4 anatomical structures. Block size 8. (b) Values greater than 0.6 . . . . .	20
4	(a) Bhattacharyya distances for the 6 combinations of 4 anatomical structures. Block size 16. (b) Values greater than 5 . . . . .	21
5	Classification of a human knee data based on (a) The first 11 co-occurrence matrix features listed in the table above, misclassification rate 0.4051, (b) gray-level data plus features 2, 14, 15, 3, 4 and 5, misclassification 0.1698, (c) grey level thresholding of the data only, misclassification 0.2244.	26
6	Comparison of the misclassification rates. . . . .	26

## List of Tables

1	Notation . . . . .	5
2	Textural Features: . . . . .	7
3	Some characteristics of the co-occurrence matrix . . . . .	8
4	Features with highest Bhattacharyya distance measure . . . . .	25

# 1 The Co-occurrence Matrix

The co-occurrence matrix defines the joint occurrences of grey tones (or ranges of tones) and is constructed by analysing the grey levels of neighbouring pixels for a given image  $\mathcal{I}$ . Let the original image  $\mathcal{I}$  with dimensions for rows and columns  $N_r \times N_c$  be quantised to  $N_g$  grey levels. The co-occurrence matrix will be a symmetric  $N_g \times N_g$  matrix that will describe the number of co-occurrences of grey levels in a certain orientation and a certain pixel distance. The unnormalised co-occurrence matrix entry  $P(i, j, G, \theta)$  records the number of times that grey levels  $i$  and  $j$  at a neighbouring distance  $d$  in the orientation  $\theta$  jointly occur. For example, if  $L_c = 1, 2, \dots, N_c$  and  $L_r = 1, 2, \dots, N_r$  are the horizontal and vertical coordinates of an image  $\mathcal{I}$ , and  $G = 1, 2, \dots, N_g$  the set of quantised grey levels, then the values of the unnormalised co-occurrence matrix  $P(i, j)$  within a distance  $d = 1$  and  $\theta = 135^\circ$  is given by:

$$P(i, j, 1, 135^\circ) = \#\{((k, l), (m, n)) \in (L_r \times L_c) \times (L_r \times L_c) \mid (k - m = 1, l - n = 1), \mathcal{I}(k, l) = i, \mathcal{I}(m, n) = j\} \quad (1)$$

where  $\#$  denotes the number of elements in the set. In other words, the matrix will be formed counting the number of times that to pixels with values  $i, j$  appear contiguous in the direction down-right (south-east).

In this way, a co-occurrence matrix is able to measure local grey level dependence: textural coarseness and directionality. For example, in coarse images, the grey level of the pixels change slightly with distance, while for fine textures the levels change rapidly. From this matrix different features like *entropy*, *uniformity*, *maximum probability*, *contrast*, *correlation*, *difference moment*, *inverse difference moment*, *correlation* can be calculated [4]. It is assumed that all the texture information is contained in this matrix. Some of the features determine the presence of a certain degree of organisation, but others measure the complexity of the grey level transitions, and therefore are more difficult to identify. The textural features <sup>1</sup> as defined in [4] and [3] are presented in tables 1, 2.

Any single matrix feature or combination can be used to represent the local regional properties but it can be difficult to predict which combination will help discriminate regions without some experimentation.

The major disadvantage of the co-occurrence matrix is that its dimensions will depend on the number of grey levels. In many cases, the grey levels are quantised to reduce the computational cost and information is lost inevitably. Otherwise, the computational burden is huge. To keep computation tractable, the grey levels are quantised,  $d$  is restricted to a small neighbourhood and a limited number of angles  $\theta$  are chosen. The images are normally processed by block of a certain size  $4 \times 4$ ,  $8 \times 8$ ,  $16 \times 16$  and they have an overlap which allows for rapid computation of the matrix [1].

---

<sup>1</sup>There are slight differences in the features presented in both texts, notice for instance that Contrast and Correlation are sometimes equivalently displayed as:  
 $f_2 = \sum_{i=1}^{N_g} \sum_{j=1}^{N_g} |i - j|^k p(i, j)$ ,  $f_3 = \sum_{i=1}^{N_g} \sum_{j=1}^{N_g} \frac{(i - \mu)(j - \mu)p(i, j)}{\sigma^2}$

Table 1: Notation

$\frac{p(i, j)}{N_g}$	$(i, j)$ th entry in a normalised matrix.
$p_x(i) = \sum_{j=1}^{N_g} p(i, j)$	Number of distinct grey levels of the quantised image.
$p_y(j) = \sum_{i=1}^{N_g} p(i, j)$	$i$ th entry in the marginal-probability matrix by summing the rows.
$p_{x+y}(k) = \sum_{i=1}^{N_g} \sum_{j=1}^{N_g} p(i, j),$ $i+j=k$	$j$ th entry in the marginal-probability matrix by summing the columns.
$p_{x-y}(k) = \sum_{i=1}^{N_g} \sum_{j=1}^{N_g} p(i, j),$ $ i-j =k$	$k = 2, 3, \dots, 2N_g$ .
$HXY = - \sum_{i=1}^{N_g} \sum_{j=1}^{N_g} p(i, j) \log\{p(i, j)\}$	$k = 0, 1, \dots, N_g - 1$ .
$HX = - \sum_{i=1}^{N_g} p_x(i) \log\{p_x(i)\}$	Entropy of $p(i, j)$
$HY = - \sum_{j=1}^{N_g} p_y(j) \log\{p_y(j)\}$	Entropy of $p_x(i)$
$HXY1 = - \sum_{i=1}^{N_g} \sum_{j=1}^{N_g} p(i, j) \log\{p_x(i)p_y(j)\}$	Entropy of $p_y(j)$
$HXY2 = - \sum_{i=1}^{N_g} \sum_{j=1}^{N_g} p_x(i)p_y(j) \log\{p_x(i)p_y(j)\}$	
$Q(i, j) = \sum_k \frac{p(i, k)p(j, k)}{p_x(i)p_y(j)}$	

Even with these restrictions, the number of features can be very high and a selection method is required. If 4 angles are selected, the with 15 textural features the space will be of 60 features for every distance  $d$ , if  $d = 1, 2, 3$ , the feature space will have dimensionality of 180.

The *Bhattacharyya distance* [2] is a good way of selecting features based on how discriminant a pair of features can be. For a thorough description of the use of the Bhattacharyya distance and the Bhattacharyya Space see [5].

The rest of the report is organised as follows. A series of different binary and natural textures were analysed, for all of them the co-occurrence matrix was calculated. For the binary patterns this matrix is a  $2 \times 2$  matrix since there are only two gray levels present. For the natural textures the matrices were  $32 \times 32$ . The next section shows the features when calculated for separate blocks of the natural texture examples. These were the used to calculate the Bhattacharyya distance pairs between the different human tissues. Finally the knee data of figure 1 is classified with different features and the misclassification is calculated.

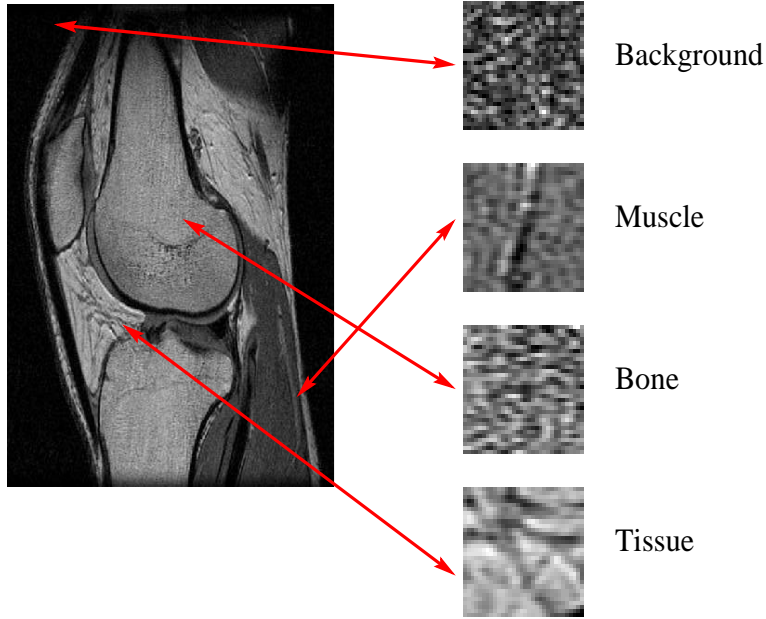


Figure 1: Human knee MRI and four selected regions.

## 2 Synthetic and Natural Textures

### 2.1 Guide to the Textures and their Results

The textures analysed were:

1. 16 binary synthetic images that range from noise (1,16), horizontal (2), vertical (3), diagonal with different frequencies and orientations (6-15) and checkerboards (4,5).
2. 4 Natural textures: four different anatomical structures were extracted from a MRI set of a human knee: *background*, *muscle*, *bone*, *tissue*. Figure 1 shows the original image and the position from where they were extracted.

For all the textures, the co-occurrence matrix was calculated for 4 different orientations  $\theta = \{0, \frac{\pi}{4}, \frac{\pi}{2}, \frac{3\pi}{4}\}$  and three distances  $d = \{1, 2, 3\}$ . When observing the matrices, it is important to observe which textures are invariant to the distance or the angle. Some general characteristics are summarised in the following table.

Table 2: Textural Features:

$$\text{Angular Second Moment (Uniformity)} \quad f_1 = \sum_{i=1}^{N_g} \sum_{j=1}^{N_g} \{p(i, j)\}^2 \quad (2)$$

$$\text{Element Difference Moment or Contrast}^1 \quad f_2 = \sum_{n=0}^{N_g-1} n^2 \left\{ \sum_{i=1}^{N_g} \sum_{j=1}^{N_g} p(i, j) \right\} \quad (3)$$

$$\text{Correlation}^1 \quad f_3 = \frac{\sum_{i=1}^{N_g} \sum_{j=1}^{N_g} (ij)p(i, j) - \mu_x \mu_y}{\sigma_x \sigma_y} \quad (4)$$

$$\text{Sum of Squares : Variance} \quad f_4 = \sum_{i=1}^{N_g} \sum_{j=1}^{N_g} (i - \mu)^2 p(i, j) \quad (5)$$

$$\text{Inverse Difference Moment} \quad f_5 = \sum_{i=1}^{N_g} \sum_{j=1}^{N_g} \frac{p(i, j)}{1 + |i - j|^2} \quad (6)$$

$$\text{Sum Average} \quad f_6 = \sum_{i=2}^{2N_g} i p_{x+y}(i) \quad (7)$$

$$\text{Sum Variance} \quad f_7 = \sum_{i=2}^{2N_g} (i - f_6)^2 p_{x+y}(i) \quad (8)$$

$$\text{Sum Entropy} \quad f_8 = - \sum_{i=2}^{2N_g} p_{x+y}(i) \log \{p_{x+y}(i)\} \quad (9)$$

$$\text{Entropy} \quad f_9 = - \sum_{i=1}^{N_g} \sum_{j=1}^{N_g} p(i, j) \log \{p(i, j)\} \quad (10)$$

$$\text{Difference Variance} \quad f_{10} = \text{Var}\{p_{x-y}(k)\} \quad (11)$$

$$\text{Difference Entropy} \quad f_{11} = - \sum_{i=0}^{N_g-1} p_{x-y}(i) \log \{p_{x-y}(i)\} \quad (12)$$

$$\text{Information Measures of Correlation} \quad f_{12} = - \frac{HXY - HXY1}{\max\{HX, HY\}} \quad (13)$$

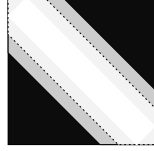
$$f_{13} = (1 - e^{-2(HXY2 - HXY)})^{\frac{1}{2}} \quad (14)$$

$$\text{Maximal Correlation Coefficient} \quad f_{14} = (\text{Second Largest Eigenvalue of } Q)^{\frac{1}{2}} \quad (15)$$

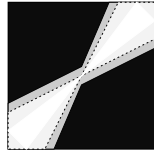
$$\text{Maximum Probability} \quad \max\{p(i, j)\} \quad (16)$$



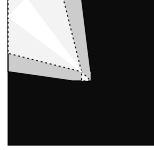
Table 3: Some characteristics of the co-occurrence matrix



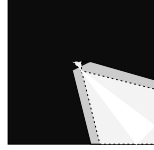
High values in the main diagonal imply uniformity in the image. That is, most transitions occur between similar levels of gray  $0 \rightarrow 0$ ,  $1 \rightarrow 1$  for the binary. *Examples:* [2  $\theta = 0, \forall d$  ], [3  $\theta = \frac{\pi}{2}, \forall d, \theta = \frac{3\pi}{4}, d = 2$ ].



High values outside the main diagonal imply abrupt changes in the grey level, from very dark to very bright  $0 \rightarrow 1$ ,  $1 \rightarrow 0$  for the binary. *Examples:* [5  $\theta = 0, d = 1$ ], [2  $\theta = \frac{\pi}{2}, d = 1, 3$ ], [3  $\theta \neq \frac{\pi}{2}, d = 1$ ], [9  $\theta \neq \frac{3\pi}{4}, d = 1$ ].



High values in the upper part imply a darker image. *Examples:* [4, 14, 15  $\forall \theta, d$ ], [17  $\theta = 0, d = 1$ ].



High values in the lower part imply a brighter image. *Examples:* [8, 9  $\theta = 0, d = 1$ ], [20  $\theta = 0, d = 1$ ].



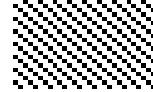



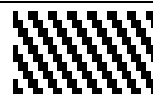



High values in the lower central region part imply an image whose transitions occur mainly between similar grey levels and whose histogram is of a Gaussian shape. *Examples:* [18  $\theta = \frac{3\pi}{4}, dd = 1$ ].



In a noisy image, the transitions between different grey levels should be balanced and it should be invariant to  $d$  and  $\theta$ , *Examples:* [1, 16], although 1 tends to be darker. The reverse, a balanced matrix, does not imply a noisy image, *Examples:* [10-13  $\theta = 0, d = 1$ ]

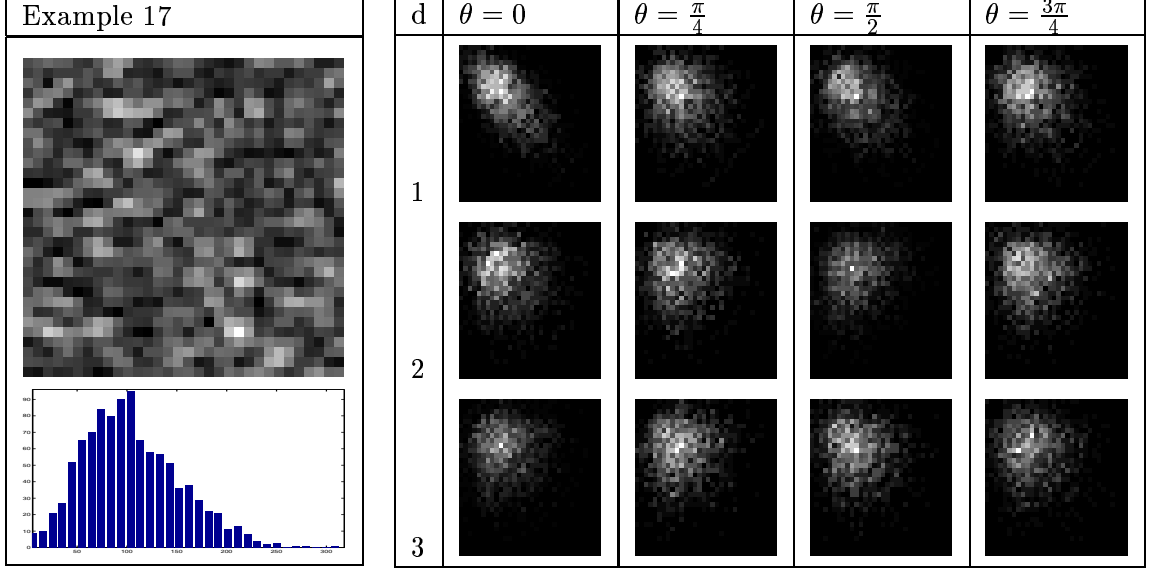
## 2.2 Co-occurrence Matrices of the Binary Textures

[illegible]

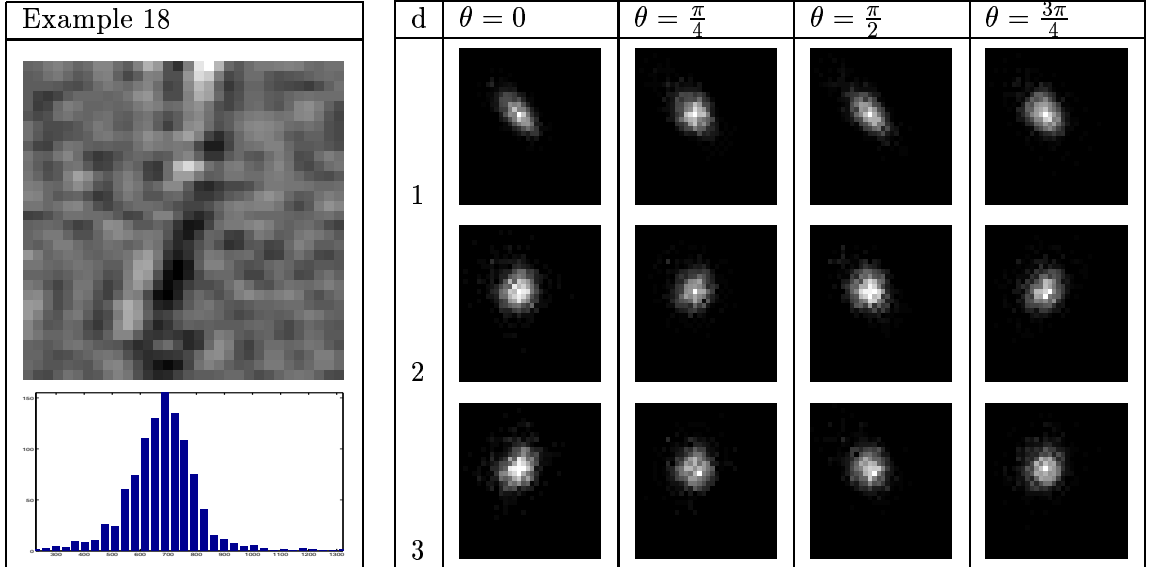
	Example	d	$\theta = 0$	$\theta = \frac{\pi}{4}$	$\theta = \frac{\pi}{2}$	$\theta = \frac{3\pi}{4}$
9		1	[ 0.000 0.334 0.334 0.333 ]	[ 0.000 0.333 0.333 0.334 ]	[ 0.000 0.334 0.334 0.333 ]	[ 0.334 0.000 0.000 0.666 ]
		2	[ 0.000 0.333 0.333 0.333 ]	[ 0.000 0.333 0.333 0.333 ]	[ 0.000 0.333 0.333 0.333 ]	[ 0.333 0.000 0.000 0.667 ]
		3	[ 0.334 0.000 0.000 0.666 ]	[ 0.334 0.000 0.000 0.666 ]	[ 0.334 0.000 0.000 0.666 ]	[ 0.334 0.000 0.000 0.666 ]
10		1	[ 0.250 0.250 0.250 0.250 ]	[ 0.501 0.000 0.000 0.499 ]	[ 0.250 0.250 0.250 0.250 ]	[ 0.000 0.500 0.500 0.000 ]
		2	[ 0.000 0.500 0.500 0.000 ]	[ 0.501 0.000 0.000 0.499 ]	[ 0.000 0.500 0.500 0.000 ]	[ 0.499 0.000 0.000 0.501 ]
		3	[ 0.250 0.250 0.250 0.250 ]	[ 0.501 0.000 0.000 0.499 ]	[ 0.250 0.250 0.250 0.250 ]	[ 0.000 0.500 0.500 0.000 ]
11		1	[ 0.250 0.250 0.250 0.250 ]	[ 0.000 0.500 0.500 0.000 ]	[ 0.250 0.250 0.250 0.250 ]	[ 0.501 0.000 0.000 0.499 ]
		2	[ 0.000 0.500 0.500 0.000 ]	[ 0.499 0.000 0.000 0.501 ]	[ 0.000 0.500 0.500 0.000 ]	[ 0.501 0.000 0.000 0.499 ]
		3	[ 0.250 0.250 0.250 0.250 ]	[ 0.000 0.500 0.500 0.000 ]	[ 0.250 0.250 0.250 0.250 ]	[ 0.501 0.000 0.000 0.499 ]
12		1	[ 0.250 0.250 0.250 0.250 ]	[ 0.129 0.371 0.371 0.129 ]	[ 0.379 0.121 0.121 0.379 ]	[ 0.371 0.129 0.129 0.370 ]
		2	[ 0.000 0.500 0.500 0.000 ]	[ 0.249 0.250 0.250 0.251 ]	[ 0.250 0.250 0.250 0.250 ]	[ 0.251 0.250 0.250 0.249 ]
		3	[ 0.250 0.250 0.250 0.250 ]	[ 0.378 0.121 0.121 0.380 ]	[ 0.129 0.371 0.371 0.129 ]	[ 0.121 0.379 0.379 0.120 ]
13		1	[ 0.250 0.250 0.250 0.250 ]	[ 0.371 0.129 0.129 0.370 ]	[ 0.379 0.121 0.121 0.379 ]	[ 0.129 0.371 0.371 0.129 ]
		2	[ 0.000 0.500 0.500 0.000 ]	[ 0.251 0.250 0.250 0.249 ]	[ 0.250 0.250 0.250 0.250 ]	[ 0.249 0.250 0.250 0.251 ]
		3	[ 0.250 0.250 0.250 0.250 ]	[ 0.121 0.379 0.379 0.120 ]	[ 0.129 0.371 0.371 0.129 ]	[ 0.378 0.121 0.121 0.380 ]
14		1	[ 0.500 0.250 0.250 0.000 ]	[ 0.688 0.062 0.062 0.187 ]	[ 0.500 0.250 0.250 0.000 ]	[ 0.566 0.184 0.184 0.067 ]
		2	[ 0.500 0.250 0.250 0.000 ]	[ 0.626 0.125 0.125 0.124 ]	[ 0.625 0.125 0.125 0.125 ]	[ 0.624 0.125 0.125 0.126 ]
		3	[ 0.500 0.250 0.250 0.000 ]	[ 0.564 0.187 0.187 0.062 ]	[ 0.500 0.250 0.250 0.000 ]	[ 0.691 0.058 0.058 0.193 ]
15		1	[ 0.500 0.250 0.250 0.000 ]	[ 0.563 0.187 0.187 0.062 ]	[ 0.500 0.250 0.250 0.000 ]	[ 0.684 0.067 0.067 0.183 ]
		2	[ 0.500 0.250 0.250 0.000 ]	[ 0.624 0.125 0.125 0.126 ]	[ 0.625 0.125 0.125 0.125 ]	[ 0.626 0.125 0.125 0.124 ]
		3	[ 0.500 0.250 0.250 0.000 ]	[ 0.687 0.062 0.062 0.188 ]	[ 0.500 0.250 0.250 0.000 ]	[ 0.558 0.192 0.192 0.058 ]
16		1	[ 0.244 0.247 0.247 0.261 ]	[ 0.236 0.260 0.260 0.245 ]	[ 0.248 0.249 0.249 0.254 ]	[ 0.264 0.232 0.232 0.272 ]
		2	[ 0.244 0.248 0.248 0.259 ]	[ 0.241 0.255 0.255 0.249 ]	[ 0.248 0.249 0.249 0.254 ]	[ 0.246 0.252 0.252 0.251 ]
		3	[ 0.244 0.251 0.251 0.254 ]	[ 0.222 0.275 0.275 0.227 ]	[ 0.250 0.245 0.245 0.260 ]	[ 0.241 0.255 0.255 0.249 ]

### 2.3 Co-occurrence Matrices of the Knee Texture Examples

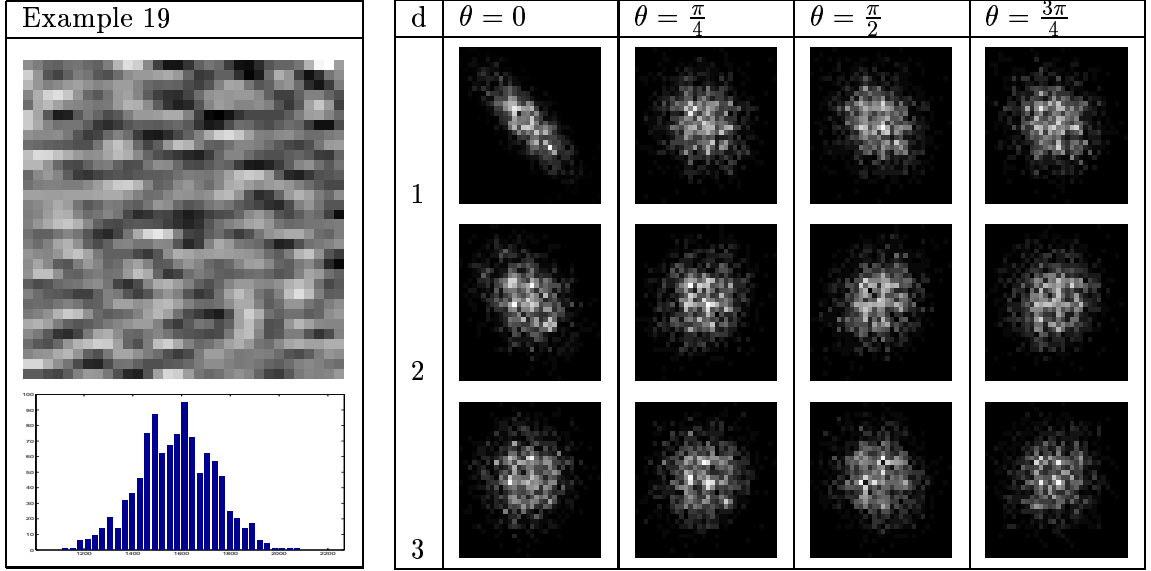
Example 17, a sample of the Background. The distribution of the co-occurrence matrix suggest a highly noisy nature with a skew towards the darker regions. There is a certain tendency to be more uniform in the horizontal direction ( $\theta = 0$ ) at a distance of  $d = 1$  which is the only matrix that is significantly different from the rest of the set.



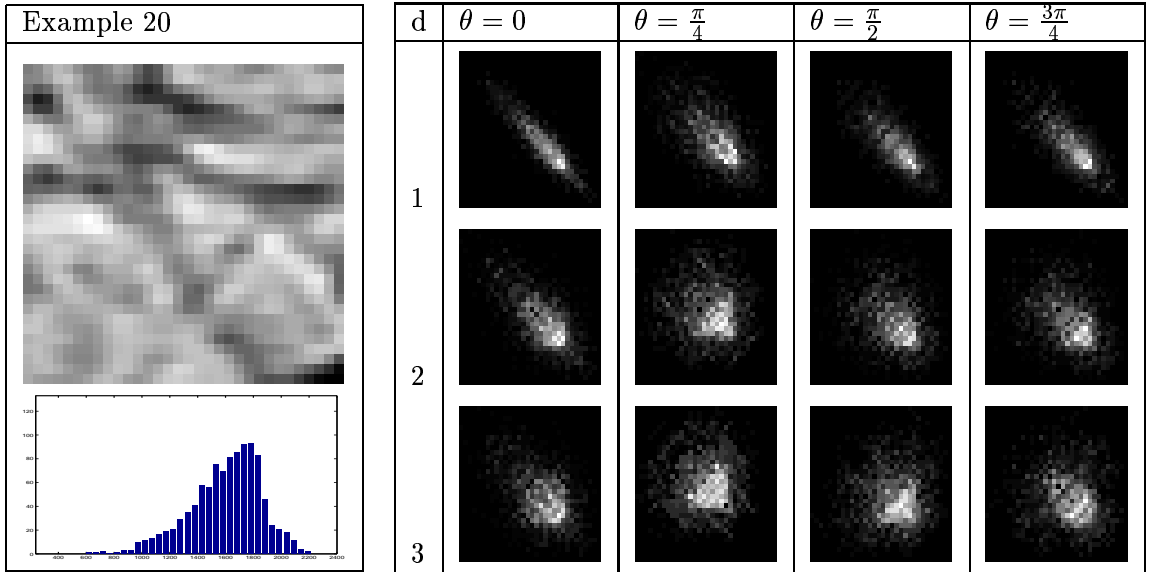
Example 18, a sample of muscle. The co-occurrence matrix is highly concentrated in the central region, the middle grey levels and there is a lower spread compared with the background. A vertical structure can be observed, this in turn gives a certain vertical and horizontal uniformity, only at distance  $d = 1$ .



Example 19, a sample of bone. The nature of the bone is highly noisy as it can be observed from the matrices, but, compared with the background, there is no skew towards dark or bright. As in the case of the muscle there is certain horizontal uniformity, but not vertical.



Example 20, a sample of tissue. The distribution is skewed towards the brighter levels. The tissue presents several major structures with a  $135^\circ$  orientation, this makes the  $\theta = \frac{\pi}{4}$  matrix to be more dispersed than the other orientations for distance  $d = 1$ . As the distance increases the matrices spread towards a noisy configuration.



### 3 Feature Spaces by blocks for Knee Textures

In this section, the co-occurrence matrix was calculated for blocks of different sizes:  $4 \times 4$ ,  $8 \times 8$ ,  $16 \times 16$ . For every matrix at every block, the value corresponding to the 15 features was and arranged into a new matrix of feature values. These are displayed graphically. It is important to notice the four parameters that modify the results:

- **Angle** A change in the orientation can result in a very different feature value.  
*Examples* Background feature 15, block size  $4 \times 4$ , Bone feature 15, block size  $16 \times 16$ , Tissue feature 5, block size  $8 \times 8$ .
- **Block size** *Examples* Background feature 2, block size  $4 \times 4$  and  $8 \times 8$ , Background feature 14, block size  $4 \times 4$ ,  $8 \times 8$  and  $16 \times 16$ .
- **Feature** The features result into very different values for any angle and any block size. A case where there are several different feature values is the Tissue block size  $16 \times 16$  where in some cases the lower-right corner is highlighted f1, in others is dark f2, and in others f14 all the image appears uniform f14,  $\theta = \frac{3\pi}{4}$ .
- **Anatomical Structure** This will be easier to appreciate in the section 3.3 where the whole MRI is processed by blocks and then the contrast between structures will appear in the image.

The values obtained from the features, are, by themselves, not very useful. Nevertheless, important information can be extracted if a discrimination measure is used for feature selection. Feature selection is a critical step in classification since not all features derived from the co-occurrence matrix (or any other methodology) have the same discrimination power. With the samples used as training data, a discrimination process was proposed in [5] which allows the selection of a reduced set of features based on the discrimination power of the individual features taken independently. In order to obtain a quantitative measure of *how separable* two classes are, a distance measure is required. The *Bhattacharyya distance* [2] is a suitable measure. The variance and mean of each class are computed to calculate a distance in the following way:

$$B(a, b) = \frac{1}{4} \ln \left\{ \frac{1}{4} \left( \frac{\sigma_a^2}{\sigma_b^2} + \frac{\sigma_b^2}{\sigma_a^2} + 2 \right) \right\} + \frac{1}{4} \left\{ \frac{(\mu_a - \mu_b)^2}{\sigma_a^2 + \sigma_b^2} \right\} \quad (17)$$

where:  $B(a, b)$  is the Bhattacharyya distance between  $a - th$  and  $b - th$  classes,  $\sigma_a$  is the variance of the  $a - th$  class,  $\mu_a$  is the mean of the  $a - th$  class, and  $a, b$  are two different training classes.

The Mahalanobis distance used in Fisher LDA is a particular case of the Bhattacharyya, when the variances of the two classes are equal, this would eliminate the first term of the distance. The second term, on the other hand will be zero if the means are equal and is inversely proportional to the variances.

The following three subsections will describe:

- 3.1 The individual feature spaces for the samples or training data are presented. By themselves they are not very explicit, but the Bhattacharyya Spaces presented next can be extracted and from them the most discriminant features.

3.2 Bhattacharyya Spaces. The Bhattacharyya distance values were calculated for the pairs [Background-Muscle], [Background-Bone], [Background-Tissue], [Muscle-Bone], [Muscle-Tissue], [Bone-Tissue], for each of the 15 features. For robustness, 4 different samples were selected from the original MRI. In order to select the most discriminant features, the associated thresholded version are presented next to each block size space. One interesting observation is that for block size  $16 \times 16$  the distances for the pair [Muscle-Tissue] for the 4 examples is considerably smaller than for the other block sizes.

3.3 When the features are calculated by blocks over the whole image, the resulting new images are much more revealing. The features were calculated with a distance  $d = 1$  and block size  $8 \times 8$ . It should be noted how each feature can reveal certain details of the image. For example,

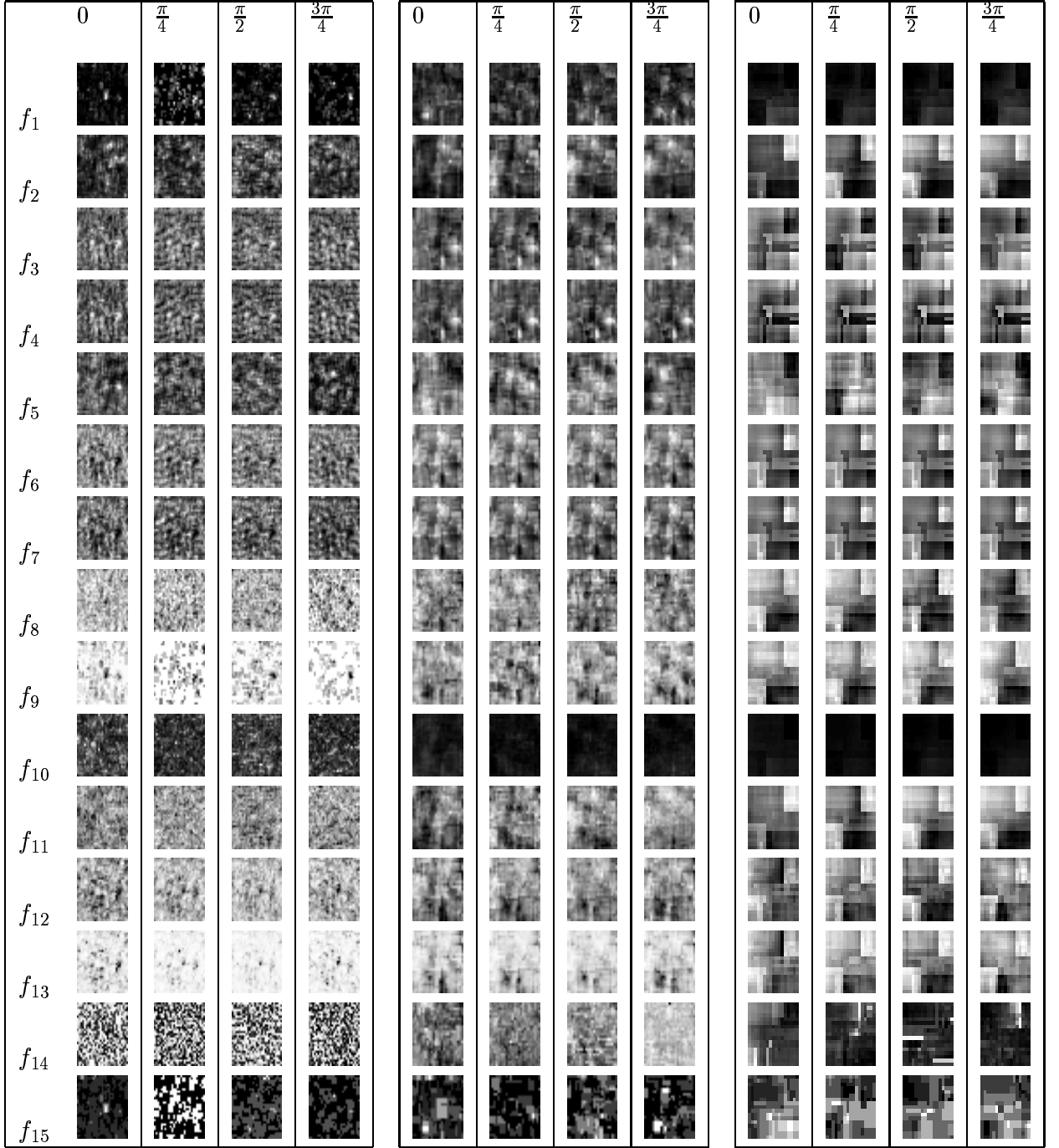
- feature 2  $\theta = \{\frac{\pi}{2}, \frac{3\pi}{4}\}$  filters out the tissue and partly the muscle, while the bone and background are present.
- Features 3 and 4 highlight the edges of the knee,
- Feature 7 creates a darker region for the background and brighter for all the other structures.
- The meniscus is highlighted in feature 10  $\theta = 0$ .

### 3.1 Example 17 : Background

Block size =  $4 \times 4$

Block size =  $8 \times 8$

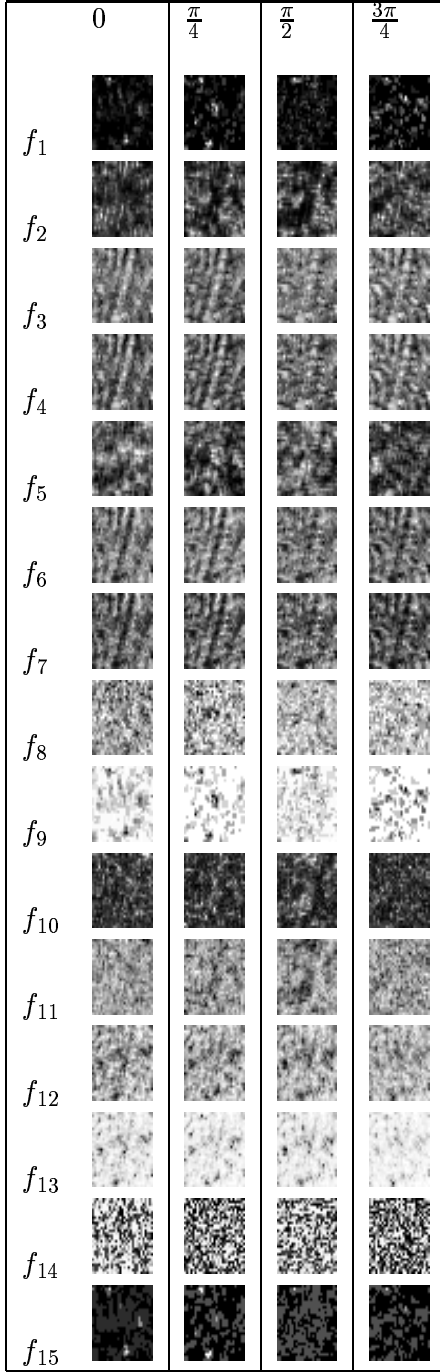
Block size =  $16 \times 16$



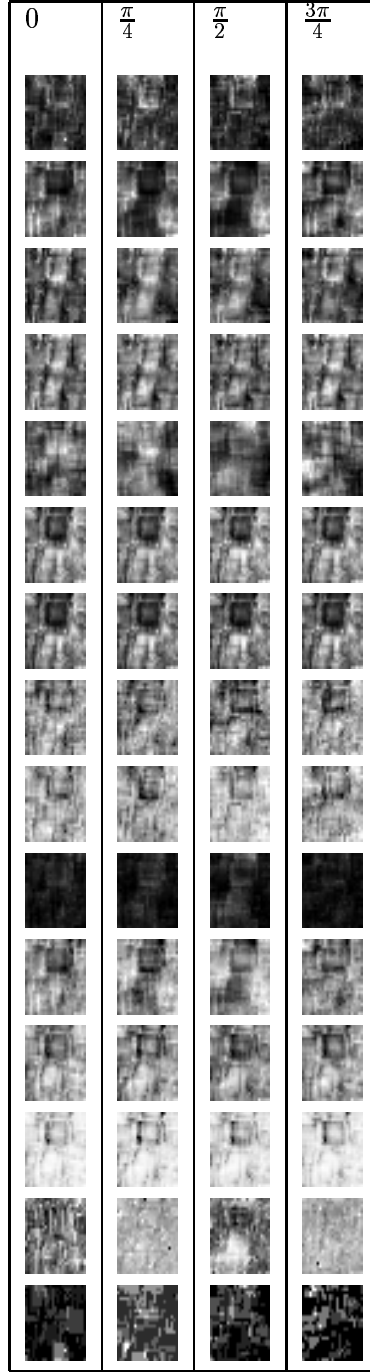


### 3.2 Example 18 : Muscle

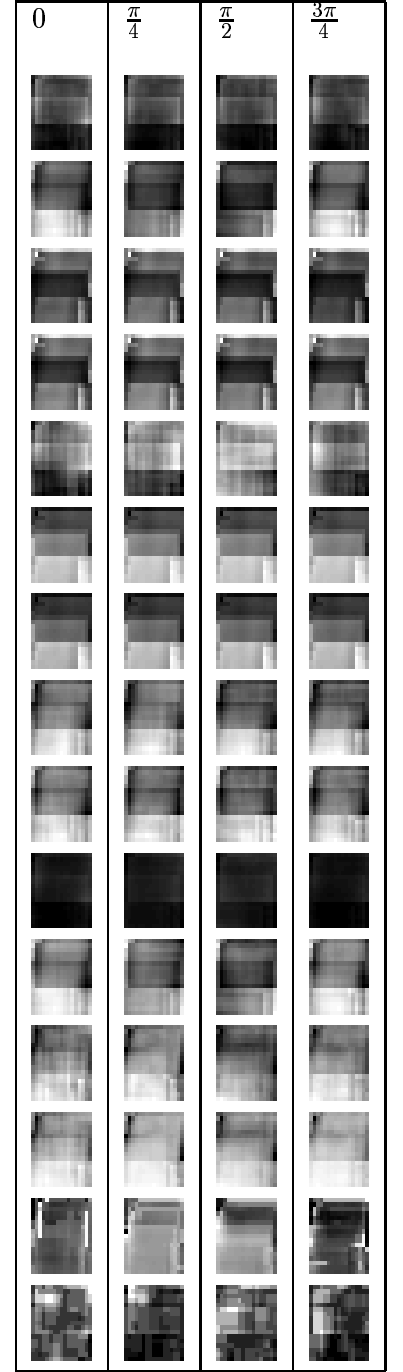
Block size =  $4 \times 4$



Block size =  $8 \times 8$



Block size =  $16 \times 16$

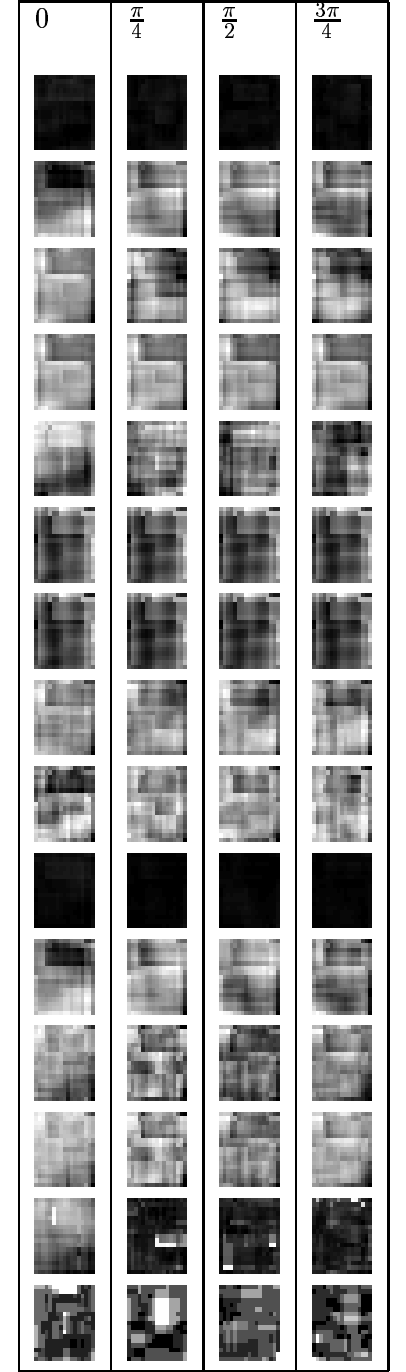
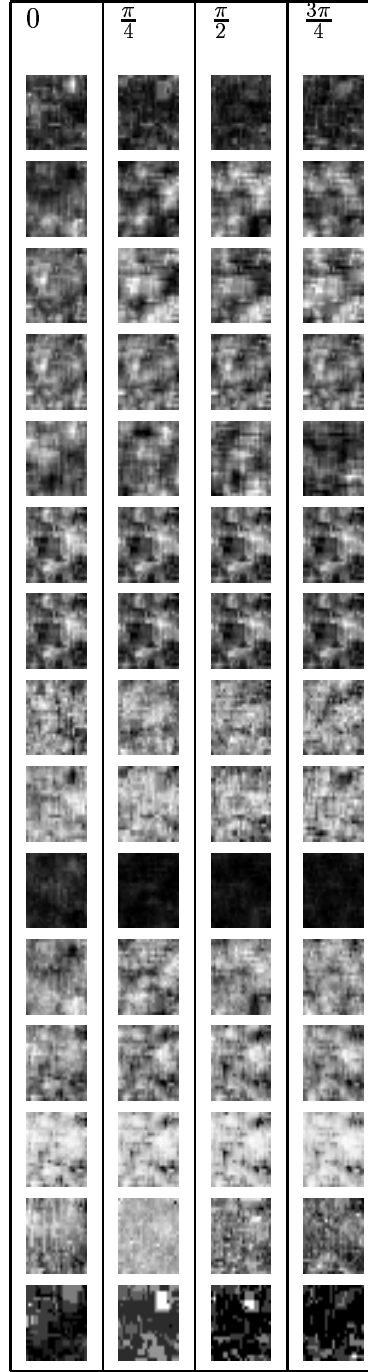
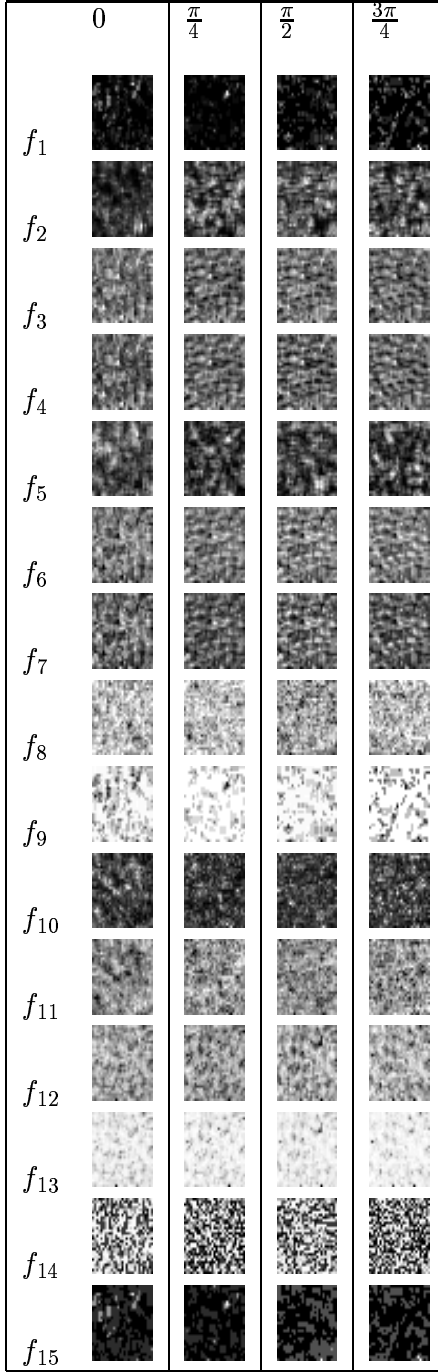


### 3.3 Example 19 : Bone

Block size =  $4 \times 4$

Block size =  $8 \times 8$

Block size =  $16 \times 16$



### 3.4 Example 20 : Tissue

Block size =  $4 \times 4$

	0	$\frac{\pi}{4}$	$\frac{\pi}{2}$	$\frac{3\pi}{4}$
$f_1$				
$f_2$				
$f_3$				
$f_4$				
$f_5$				
$f_6$				
$f_7$				
$f_8$				
$f_9$				
$f_{10}$				
$f_{11}$				
$f_{12}$				
$f_{13}$				
$f_{14}$				
$f_{15}$				

Block size =  $8 \times 8$

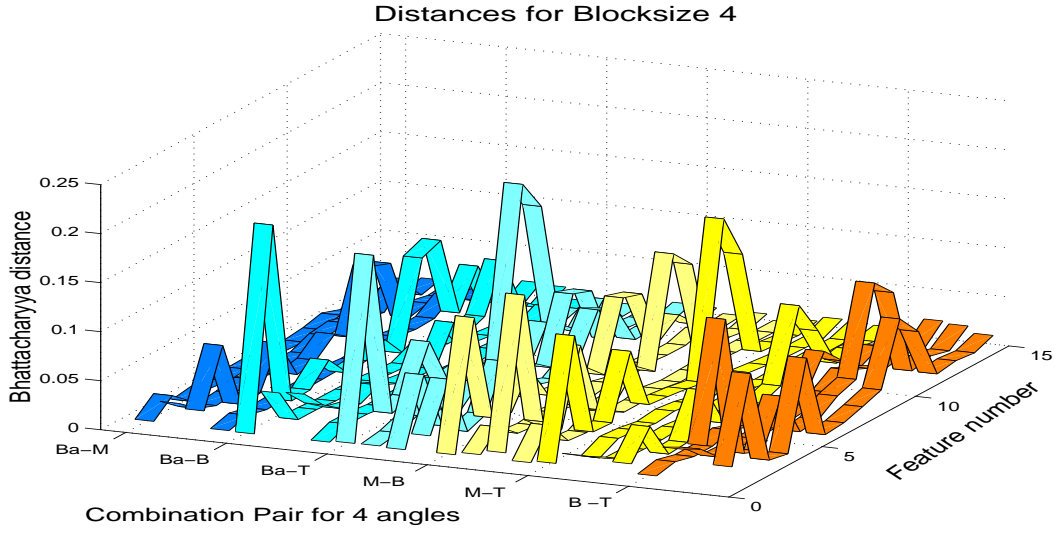
	0	$\frac{\pi}{4}$	$\frac{\pi}{2}$	$\frac{3\pi}{4}$
$f_1$				
$f_2$				
$f_3$				
$f_4$				
$f_5$				
$f_6$				
$f_7$				
$f_8$				
$f_9$				
$f_{10}$				
$f_{11}$				
$f_{12}$				
$f_{13}$				
$f_{14}$				
$f_{15}$				

Block size =  $16 \times 16$

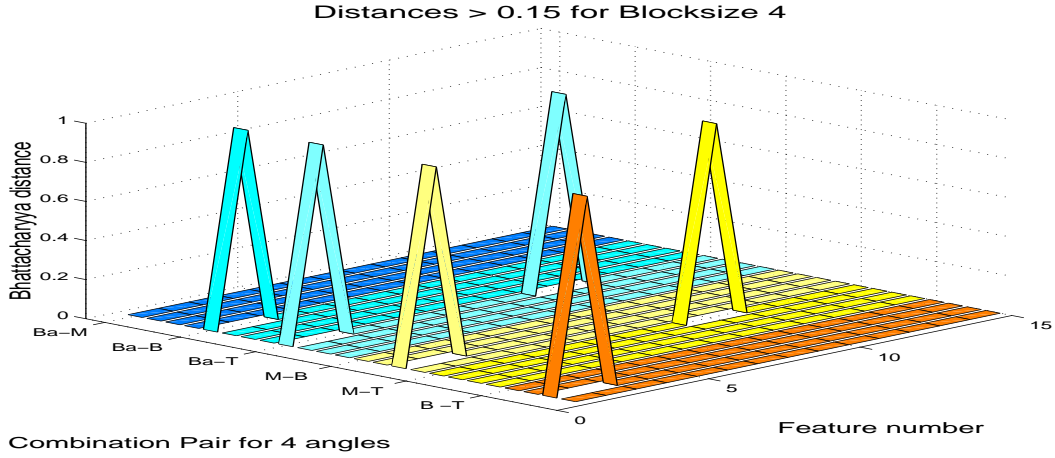
	0	$\frac{\pi}{4}$	$\frac{\pi}{2}$	$\frac{3\pi}{4}$
$f_1$				
$f_2$				
$f_3$				
$f_4$				
$f_5$				
$f_6$				
$f_7$				
$f_8$				
$f_9$				
$f_{10}$				
$f_{11}$				
$f_{12}$				
$f_{13}$				
$f_{14}$				
$f_{15}$				

### 3.5 Bhattacharyya distances for pairs of data

Key to the pairs: Ba-M Background-Muscle Ba-B Background-Bone  
Ba-T Background-Tissue M-B Muscle-Bone  
M-T Muscle-Tissue B-T Bone-Tissue



(a)



(b)

Figure 2: (a) Bhattacharyya distances for the 6 combinations of 4 anatomical structures. Block size 4. (b) Values greater than 0.15

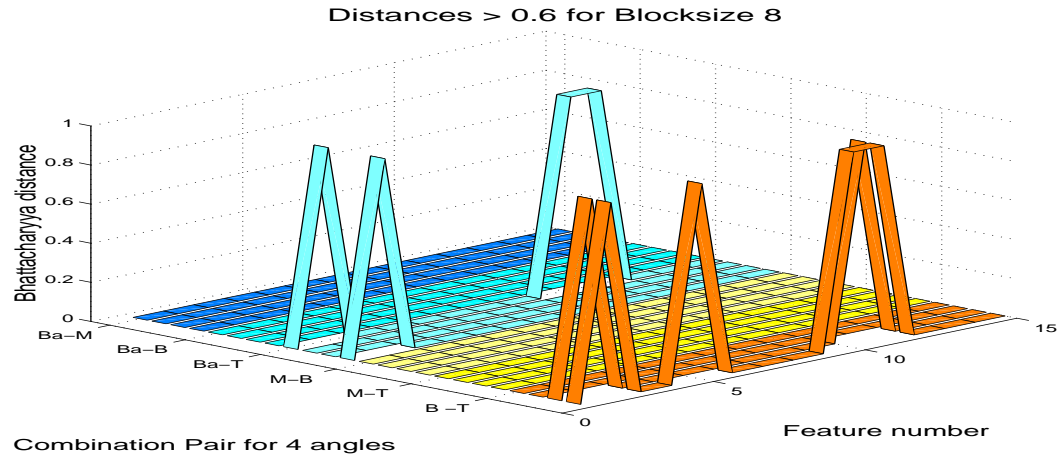
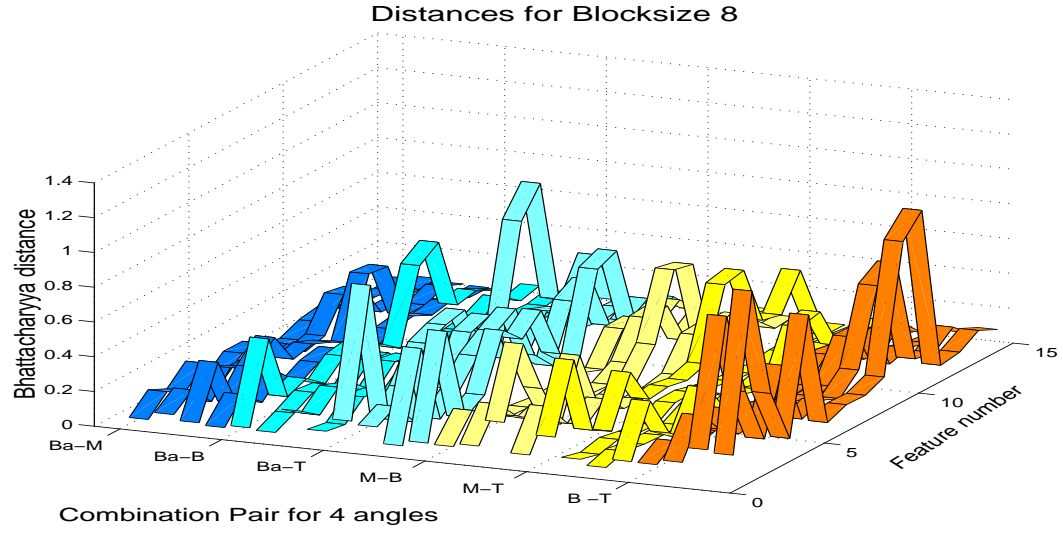


Figure 3: (a) Bhattacharyya distances for the 6 combinations of 4 anatomical structures. Block size 8. (b) Values greater than 0.6

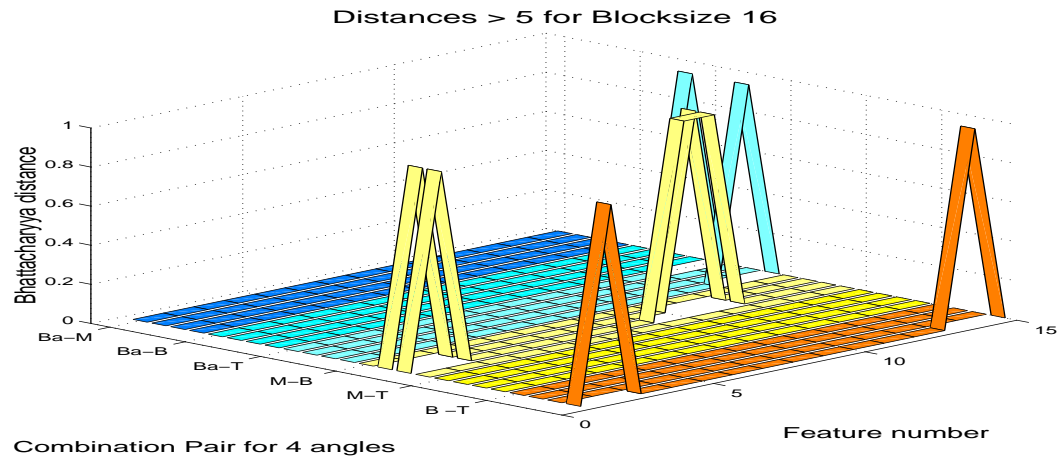
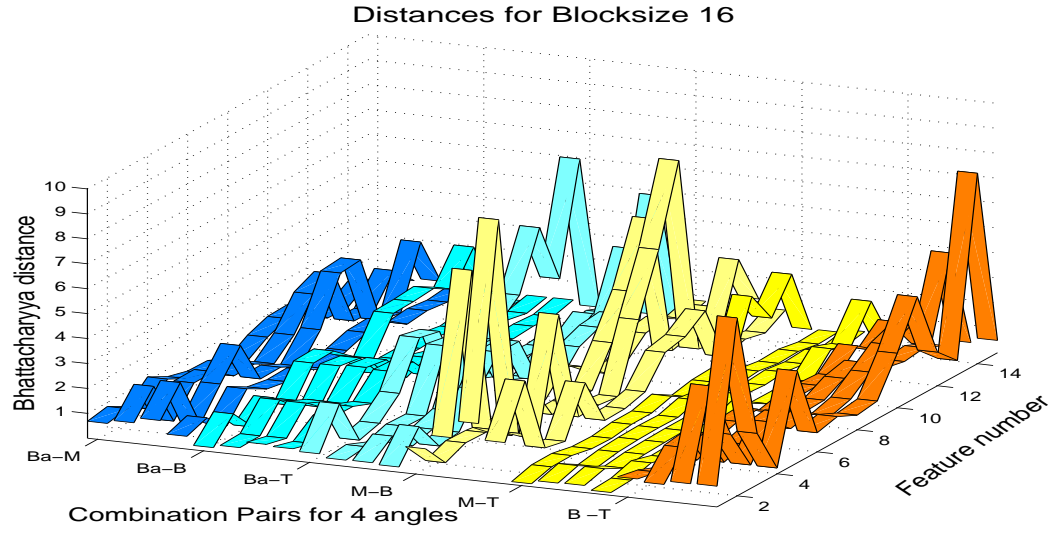
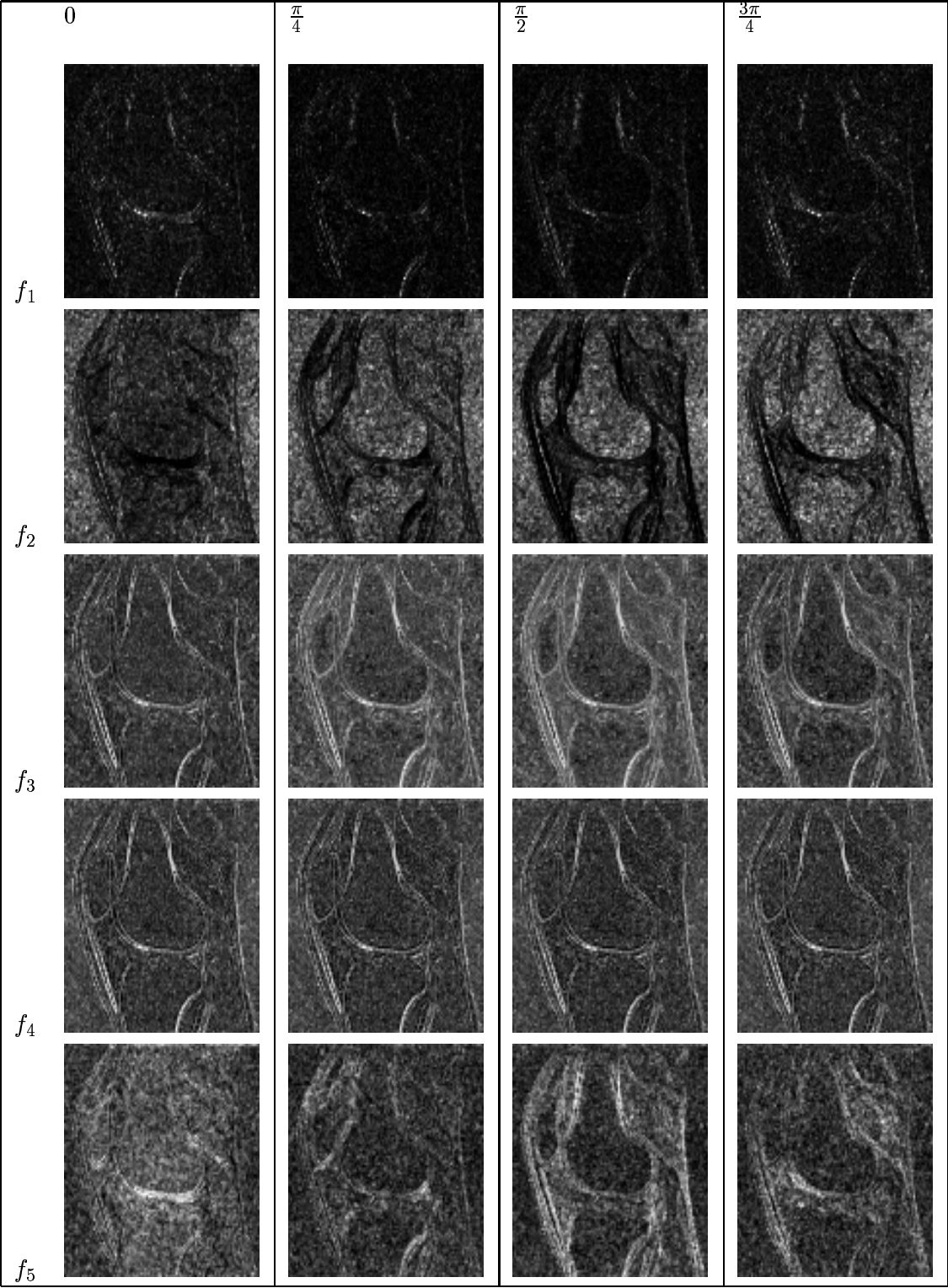
















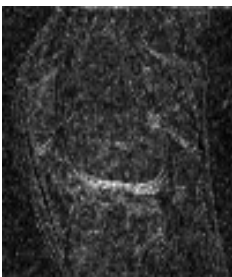
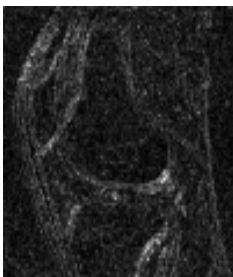
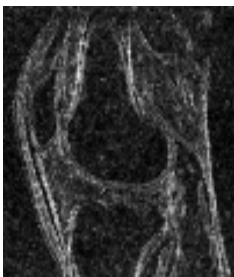



Figure 4: (a) Bhattacharyya distances for the 6 combinations of 4 anatomical structures. Block size 16. (b) Values greater than 5







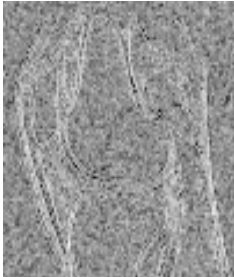

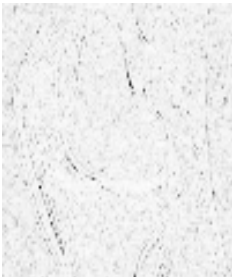
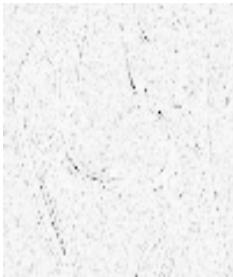
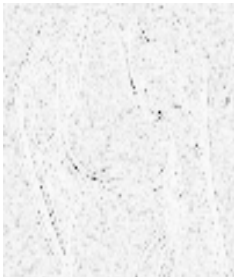
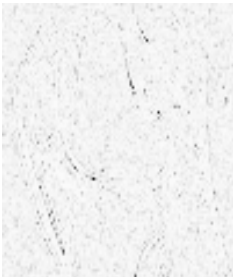
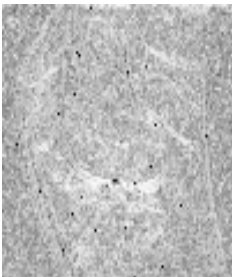
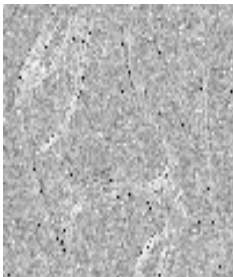
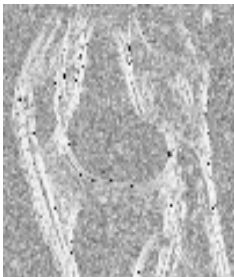
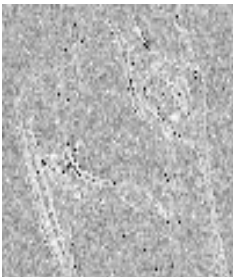

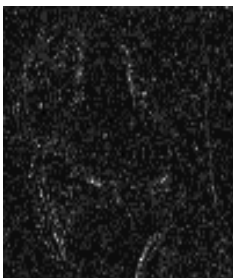

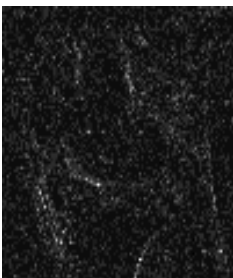
### 3.6 15 Features of Matrices by blocks from the Human Knee MRI





	0	$\frac{\pi}{4}$	$\frac{\pi}{2}$	$\frac{3\pi}{4}$
$f_6$				
$f_7$				
$f_8$				
$f_9$				
$f_{10}$				



	0	$\frac{\pi}{4}$	$\frac{\pi}{2}$	$\frac{3\pi}{4}$
$f_{11}$				
$f_{12}$				
$f_{13}$				
$f_{14}$				
$f_{15}$				

## 4 Classification Results based on Bhattacharyya distances for pairs of data

In order to classify the human knee data a series of features of the Co-occurrence Matrix were selected. The matrix was obtained with a block size = 8 and distance  $d = 1$  iteratively over the image, and the features with higher Bhattacharyya distance measure were used as training sets for a *k-means* classification. The first 10 features selected are presented in the table 4.

Table 4: Features with highest Bhattacharyya distance measure

1	$f_2(\theta = 0)$
2	$f_2(\theta = \frac{\pi}{2})$
3	$f_2(\theta = \frac{3\pi}{4})$
4	$f_5(\theta = \frac{3\pi}{4})$
5	$f_{10}(\theta = 0)$
6	$f_{10}(\theta = \frac{\pi}{2})$
7	$f_{10}(\theta = \frac{3\pi}{4})$
8	$f_{11}(\theta = 0)$
9	$f_{11}(\theta = \frac{\pi}{2})$
10	$f_{11}(\theta = \frac{3\pi}{4})$
11	$f_5(\theta = \frac{\pi}{2})$

The features were used as the input for the classifier and the means of the training samples were the initial values of the means for the four classes: *background*, *muscle*, *bone*, *tissue*. The error rate obtained was close to 40%. To improve the misclassification, the original grey-level image data was included as one of the features for classification. The mean values used for the four classes were background = 90, muscle = 700, bone = 1600 and tissue = 1650. The classification is greatly improved but some of the features do not lower the classification as they are included in the classifier. Therefore, these are ordered and classified again, this yields a minimum when only 6 features and the data are introduced to the classifier: misclassification 0.1698. If the only the data were introduced (grey level thresholding), the misclassification is 0.2244, a good classification for background and muscle but not for bone and tissue. The classified images are shown below with a graph comparing the misclassification rates.

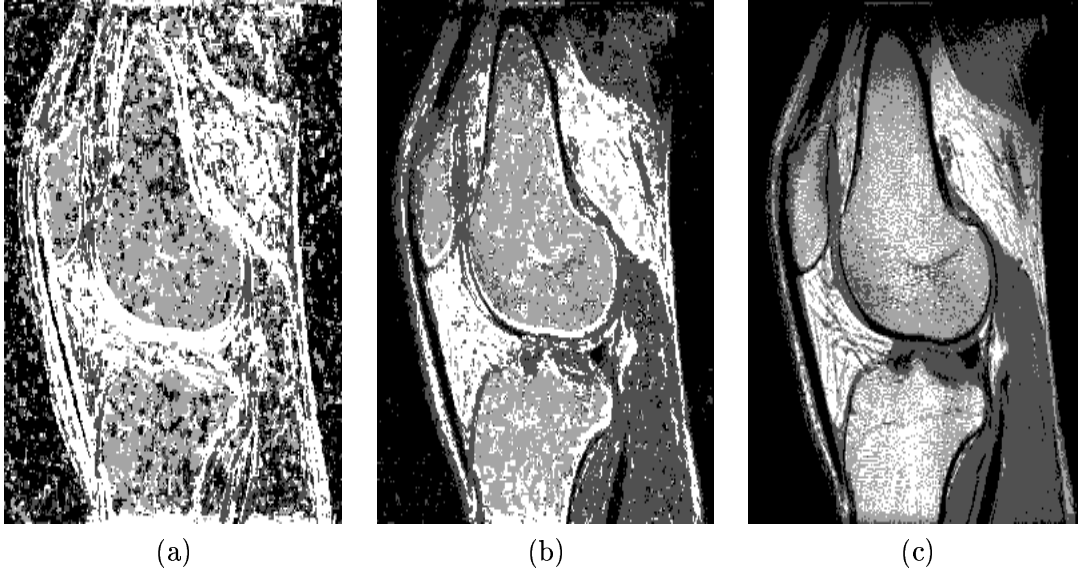


Figure 5: Classification of a human knee data based on (a) The first 11 co-occurrence matrix features listed in the table above, misclassification rate 0.4051, (b) gray-level data plus features 2, 14, 15, 3, 4 and 5, misclassification 0.1698, (c) grey level thresholding of the data only, misclassification 0.2244.

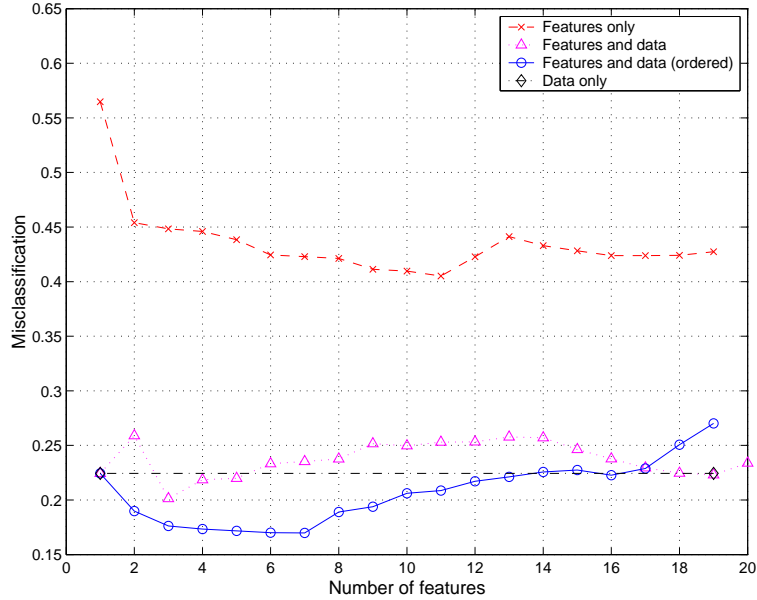


Figure 6: Comparison of the misclassification rates.

## References

- [1] L. Alparonte, F. Argenti, and G Benelli. Fast calculation of co-occurrence matrix parameters for image segmentation. *Electronics Letters*, 26(1):23–24, 4 January 1990.
- [2] K. Fukunaga. *Introduction to Statistical Pattern Recognition*. Academic Press, 1972.
- [3] Robert M. Haralick. Statistical and structural approaches to texture. *Proceedings of the IEEE*, 67(5):786–804, 1979.
- [4] Robert M. Haralick, K. Shanmugam, and Its'hak Dinstein. Textural features for image classification. *IEEE, Transactions on Systems, Man and Cybernetics*, SMC-3(6):610–621, 1973.
- [5] C.C. Reyes-Aldasoro and A.Bhalerao. Volumetric texture description and discriminant feature selection for MRI. In *Proceedings of Information Processing in Medical Imaging*, pages 282–293, Ambleside, UK, July 2003.